Article

Not peer-reviewed version

Arabinoxylan-Based Bioplastic from Wheat Bran: A Promising Replacement for Synthetic Plastics

Md Abdur Rahim Badsha , Michael Kjelland , Chad Ulven , Khwaja Hossain *

Posted Date: 18 June 2025

doi: 10.20944/preprints202506.1515.v1

Keywords: bioplastic; wheat bran; arabinoxylan; tensile strength; biodegradability

 doi:10.20944/preprints202506.1515.v1

Article

Arabinoxylan-Based Bioplastic from Wheat Bran: A Promising Replacement for Synthetic Plastics

Md Abdur Rahim Badsha [1], Michael Kjelland [1], Chad Ulven [2] and Khwaja Hossain [1,*]

[1] Division of Science and Mathematics, Mayville State University, Mayville, ND 58257, USA; mdabdurrahim.badsha@mayvillestate.edu (M.A.R.B.); michael.kjelland@mayvillestate.edu (M.K.)
[2] Department of Mechanical Engineering, North Dakota State University, Fargo, ND 58102, USA; chad.ulven@ndsu.edu (C. U).
* Correspondence: k.hossain@mayvillestate.edu

Abstract: The milling process of wheat annually generates over 150 million tons of wheat bran (WB), which has significant potential for bioplastic production. However, the production of bioplastics from these resources has never been explored until now. WB polymer is evaluated here to produce environmentally friendly, biodegradable plastic suitable for food packaging. The biodegradable plastic films were prepared through a molding process that involved three steps: (1) extraction of arabinoxylan from wheat bran, (2) hydrolysis and plasticization with glycerol, and (3) blending with polyvinyl alcohol (PVA) in varying proportions. The resulting bioplastic exhibits competitive mechanical properties and biodegradability. Furthermore, the biodegradable plastic developed in this research contributes to agricultural waste management, the development of value-added products, and the reduction of carbon emissions incurred from plastic industries. Additionally, it can replace and reduce reliance on synthetic plastics, which are non-degradable and a source of severe environmental pollution.

Keywords: bioplastic; wheat bran; arabinoxylan; tensile strength; biodegradability

1. Introduction

The utilization of biomass recovered from inedible agricultural wastes for bioplastic production is a promising research avenue, offering significant environmental benefits within a circular economic framework

[1–4]. Bioplastics are defined as biodegradable or nonbiodegradable polymers produced from renewable or natural biological sources. However, non-biodegradable bioplastics from biomass and fossil sources fundamentally follow a linear economy model and are not considered to be sustainable. In contrast, biodegradable bioplastics are derived from biomass and support a circular economy by combining short-term biodegradability with the conversion of waste biomass into value-added products [5,6].

Bioplastics manufactured from plant biomass provide new functionalities to the resulting product, including antioxidant, antimicrobial, and nutraceutical properties [7]. During bioplastic production, biomass is typically dried and ground into powder form to reduce bacterial and enzymatic activities, helping to preserve its composition during storage [8]. Due to its lack of thermoplasticity, this dried and ground biomass cannot be directly converted into bioplastic. Therefore, several methods have been recommended for the digestion and dissolution of the biomass [2,4,9]. Among these, acidic and alkaline hydrolysis are the most used processes [2]. The resulting plant residue is plasticized with various plasticizers, including glycerol, glycol, xylitol, sorbitol, sugars, amides, urea, formamide, and ethylene-bis-formamide [10], and is blended with synthetic polymers like polyvinyl alcohol and polylactic acid to enhance both physicochemical properties and biodegradability [11].

Wheat is one of the most consumed crops in the world [12,13]. Wheat belongs to the genus *Triticum spp*. The wheat kernel contains 14.5% bran, which is removed during the milling process. A significant amount of wheat bran is produced every year and is primarily used as cattle feed. However, due to low demand and high transportation costs, 90% of the wheat bran remains in landfills, causing environmental pollution [14].

Wheat bran contains carbohydrates like cellulose, hemicellulose, and lignin, as well as proteins, minerals such as calcium and phosphorus, silica, acid detergent fibers, and ash. Numerous studies have explored the production of value-added products such as bioplastics, biochar, and others from wheat bran fiber and/or wheat bran starch [15–18]. In this study, arabinoxylan, a major polysaccharide, was extracted from wheat bran and used it for bioplastic.

Physico-mechanical properties are essential for evaluating the suitability of bioplastics as sustainable alternatives to conventional plastics. Among these properties, tensile strength, elongation at break, Young's modulus, water solubility, and thermal and chemical resistance significantly influence the functionality and application of bioplastics in fields like food packaging, agriculture, and biomedical devices [19]. For example, tensile strength and elongation provide insights into the material's ability to withstand mechanical stress and deformation, which are crucial for load-bearing or flexible packaging applications [20].

To assess these characteristics, a range of analytical techniques is employed. The Fourier-Transform Infrared Spectroscopy (FTIR) is used to detect chemical functional groups, while Scanning Electron Microscopy (SEM) reveals surface morphology and structural integrity, and tensile testing is evaluated by a Universal Testing Machine (UTM). Additionally, water contact angle (WCA) analysis helps determine hydrophilicity or hydrophobicity. Together, these techniques provide a comprehensive understanding of bioplastic performance and serve as essential tools in material design and improvement.

However, this study focuses on utilizing arabinoxylan derived from wheat bran to develop eco-friendly bioplastics, aiming to reduce the use of commercially available synthetic plastic.

2. Materials and Methods

2.1. Chemicals and Reagents

Glycerol used as a plasticizer was purchased from Thermo Scientific, USA Polyvinyl alcohol (PVA) was obtained from Thermo Scientific, USA, and potassium hydroxide (KOH) was obtained from Fisher Chemicals, Belgium. Sulfuric acid (H_2SO_4) was bought from Fisher Chemical, USA. The $CuSO_4.5H_2O$, commercially known as blue vitriol, was purchased from Fisher Scientific, Waltham, MA, USA.

2.2. Procedures

2.2.1. Wheat Bran Collection and Extraction of Arabinoxylan

Wheat bran was collected from North Dakota Mill, Grand Forks, North Dakota. Upon collecting, the wheat bran was sieved to obtain a uniform size distribution of 2-3 mm of the bran by using a Hamilton Beach blender (Model 609-4, Hamilton Beach Inc.). Arabinoxylan was extracted following the method described in our previous work [21].

2.2.2. Bioplastic Synthesis

The bioplastic synthesis was conducted using a three-step process, following a slightly modified method described by Mendes et al [22]. The first step involved extracting arabinoxylan. The second step includes hydrolysis and plasticization with glycerol. In this phase, arabinoxylan was placed in a beaker containing distilled water. The mixture was heated to 80°C for 20 minutes, after which glycerol was added as a plasticizer to enhance the flexibility and moldability of the plastic. Finally, the mixture was blended with polyvinyl alcohol (PVA) and stirred continuously at 80°C for an additional two hours until the solution was thickened and turned into a jelly-like slurry. The thick slurry solution was poured into a petri dish and dried overnight in an oven (Thermo Scientific, Heratherm OGS60, made in Germany) at 60°C. The following day, the petri dish was removed from the oven while bioplastic film was formed. The film was then allowed to cool to room temperature and pressed into sheets using a mold. During the process, a specific ratio of materials – arabinoxylan, glycerol, and polyvinyl alcohol (PVA) – was used, as detailed in Table 1.

Table 1. The composition ratio of the bioplastic blend.

Title	Wheat bran arabinoxylan (WBAX)	Polyvinyl alcohol (PVA)	Glycerol
WBAX 1:1:2	1	1	2
WBAX 1:2:1	1	2	1
WBAX 1:2:2	1	2	2
WBAX 1:2:4	1	2	4

2.3. Characterization of the Synthesized Bioplastics

2.3.1. Fourier Transform Infrared (FT-IR) Spectroscopy

FT-IR spectral analysis was conducted after extracting arabinoxylan from wheat bran. The FT-IR spectra of the bioplastic film were analyzed after casting, and after two months of the burial of the bioplastic film in soil that used for testing biodegradability. The FT-IR analysis experiment was conducted at the Department of Chemistry, University of North Dakota, USA, using an FT-IR machine model: NICOLETiS5, Thermo Scientific, USA. The spectra, recorded in the 4000–650 cm^{-1} range, displayed absorption frequency against transmittance (%). Data acquisition resulted in an incidence angle of 45°, a 2 mm sampling area, 16 background scans, an optical resolution of 0.8 cm^{-1}, and data spacing of 0.06 cm^{-1}. The degree of cationization was quantified using the following equation:

$$C = (\mathrm{I1648} - \mathrm{I1495}) / \mathrm{I1648} \times 100\% \quad (1)$$

where I_{1648} and I_{1495} represent the peak intensities at 1648 cm^{-1} and 1495 cm^{-1}, respectively.

2.3.2. Mechanical Properties

Tensile strength (TS) was determined using an Instron Model 5542, made in the USA, following ASTM D412 [23]. Bioplastic film specimens were cut to 2.7 mm in width, with an average gauge length of 50 mm, and were mounted on the testing apparatus. The tensile test was performed at a crosshead speed of 20 mm/min to evaluate the elastic modulus. Elongation at break (EAB) was calculated by assessing the ratio of the specimen's final length after failure to its original length under applied tensile stress.

2.3.3. Scanning Electron Microscope (SEM) Analysis

The surface morphology of the bioplastic was observed using high-resolution Scanning Electron Microscopy at the Department of RCA Electron Microscopy Core, North Dakota State University, USA. First, the treated plastic samples were cut with scissors and affixed to cylindrical aluminum stubs using silver paint (SPI Products, West Chester, Pennsylvania, USA). A thin conductive layer of gold was then applied to the mounted samples with a sputter coater (Cressington 108Auto, Ted Pella, Redding, California, USA). Imaging was conducted with a JEOL JSM-6490LV scanning electron microscope (JEOL USA, Inc., Peabody, Massachusetts, USA) at an accelerating voltage of 15 kV.

2.3.4. Film's Thickness Measurements

The thickness of the film samples was measured by using a digital micrometer with a sensitivity of 0.01 mm, by taking measurements at five randomly selected points. The mean thickness value was then used for subsequent mechanical and optical property analyses.

2.3.5. Film's Transparency

The transparency of the film samples was evaluated following the slightly modified method described by Mulyono et al [24]. Bioplastic films were cut into dimensions of 1 cm × 3 cm to fit the width and height of a standard cuvette. Each film sample was attached to the side of the cuvette, and a synthetic polyethylene film served as the control. Absorbance measurements were taken at a wavelength of 800 nm by using a GENESYS 10S UV-VIS Spectrophotometer, Thermo Scientific, USA, at Mayville State University. Blue vitriol solution was used for the measurement of absorption. The transmittance (%T) was then calculated using the following equation

$$\% \text{ of T} = \text{antilog}\,(2 - \text{absorbance}) \quad (2)$$

And transparency was calculated by using the following formula

$$\text{Transparency} = \frac{log\, \%\, T}{\text{b}} \quad (3)$$

Where T is the transmittance at 800 nm and b is the thickness of the bioplastic film in millimeters.

2.3.6. Film's General Appearance

The visual characteristics of the bioplastic films were evaluated through systematic observation to assess surface texture, uniformity, color, opacity, and the presence of any physical defects such as bubbles, cracks, or warping. Each sample was photographed under standardized conditions—consistent ambient lighting, neutral background, and fixed camera settings—to ensure reliable visual documentation. These images were used to compare the aesthetic and structural integrity of films prepared under different processing conditions or compositions. Visual assessment served as an initial qualitative indicator of film quality and was used alongside analytical techniques to interpret the material's overall performance and stability.

2.3.7. Water Contact Angle

The way water interacts with the surface is commonly described by two phenomena: hydrophilicity and hydrophobicity. The water contact angle (WCA) is used as a key indicator to evaluate this behavior. Over the years, extensive research has utilized this method to investigate and understand the surface properties [25–29]. In this study, the water contact angle of the synthesized film was measured to evaluate the wearability of the film. A pluggable USB 2.0 Digital Microscope (purchased from Amazon.com) was employed to capture images of water droplets placed on the surface of the film samples. A Ziploc bag and a polyethylene bag collected from local Walmart were used as a reference to compare the water contact angle of the synthesized film. The experiment was conducted at an ambient temperature of 23 °C, a needle width of 0.525 mm, and a droplet volume of 5 μL. The water contact angle was measured using ImageJ software [30]. Images were taken multiple times for each film, and the best image was selected for analysis.

2.3.8. Water Absorption Percentage

All prepared bioplastic films were cut into dimensions of 2 cm × 2 cm and oven-dried at 60 °C for 24 hours. The initial mass of each film (M_0) was recorded. The samples were then immersed in 50 mL of distilled water for 24 hours at room temperature. After immersion, the films were removed, gently wiped with Pacific Blue Select Multifold Premium 2-Ply Paper Towels by GP PRO (Georgia-Pacific) to remove surface water and weighed to determine the final mass (M_1). The water absorption percentage was calculated using the following formula:

$$\text{Water Absorption} = \frac{M1 - Mo}{Mo} \times 100\% \quad (4)$$

Where Mo and M1 are the initial (dry) mass and the water immersion mass of the film, respectively. The experiment was conducted by the modified method described by Saberi et al [31].

Preprints.org (www.preprints.org) | NOT PEER-REVIEWED | Posted: 18 June 2025 doi:10.20944/preprints202506.1515.v1

2.3.9. Effect of Acid

Accurately weighed samples of about 1.0 g of the synthesized bioplastics from arabinoxylan were immersed in sulfuric acid (H_2SO_4) solutions with concentrations of 10%, 20%, 30%, and 40%. The samples were continually dried and weighed over certain days to assess weight loss over time, and a photograph was taken after each data collection interval. The experiment was conducted by following the method described by Mostafa et al [32].

2.3.10. Effect of Alkalis

Accurately weighed samples (synthesized bioplastics from arabinoxylan) of about 1.0 g were taken by using a high-accuracy electronic balance (Denver Instruments XE-100, USA, Serial No NO111601, Max: 100g, d: 0.0001g). The plastic pieces were immersed in potassium hydroxide (KOH) solutions at varying concentrations of 10%, 20%, 30%, and 40%. The percentage of weight loss was calculated every second day for ten days, and a photograph was taken after each data collection interval.

2.3.11. Biodegradability Test

The biodegradability experiment was conducted following a modified procedures described by various researchers [32,33]. The synthesized bioplastic samples were oven-dried at 45°C for two hours and weighed on a high-accuracy electronic balance. The weighted bioplastic pieces were buried in natural soil obtained from a fallow land surrounding Mayville State University to assess biodegradation. Throughout the experiment, soil moisture content and temperatures were carefully maintained. At four-week intervals, the samples were washed, dried, and weighed to calculate the percentage of weight loss, with a photograph taken after each data collection. For the final data collection, a Scanning Electron Microscope (SEM) image and a Fourier Transform Infrared (FT-IR) spectrum were assessed obtained with a photograph for general appearance.

3. Results

3.1. Fourier Transform Infrared (FT-IR) Spectroscopy

Figure 1 shows the FT-IR spectra of arabinoxylan extracted from wheat bran and the bioplastic made from it. From figure 1(a), the characteristic spectrum for arabinoxylan was observed at 3205 cm^{-1}, 2918 cm^{-1}, and 1018 cm^{-1}, which correspond to O-H stretching, C-H stretching, and C-OH stretching of glycosidic linkages, respectively. Figure 1(b) indicates the characteristic peaks of WBAX 1:2:1 bioplastic at 3252 cm^{-1}, 2911 cm^{-1}, 1651 cm^{-1}, 1419 cm^{-1}, 1039 cm^{-1}, and 676 cm^{-1}. The broad peaks at 3252 cm^{-1} and 2911 cm^{-1} indicate the stretching vibrations of O-H and -CH respectively, confirming the interactions of different O-H groups in the arabinoxylan, glycerol, and PVA blend. The peak at 1651 cm^{-1} confirms the triglyceride linkage [34]. The peaks below 1039 cm^{-1} indicate the strong molecular hydrogen bonding of hydroxyl group.

 doi:10.20944/preprints202506.1515.v1

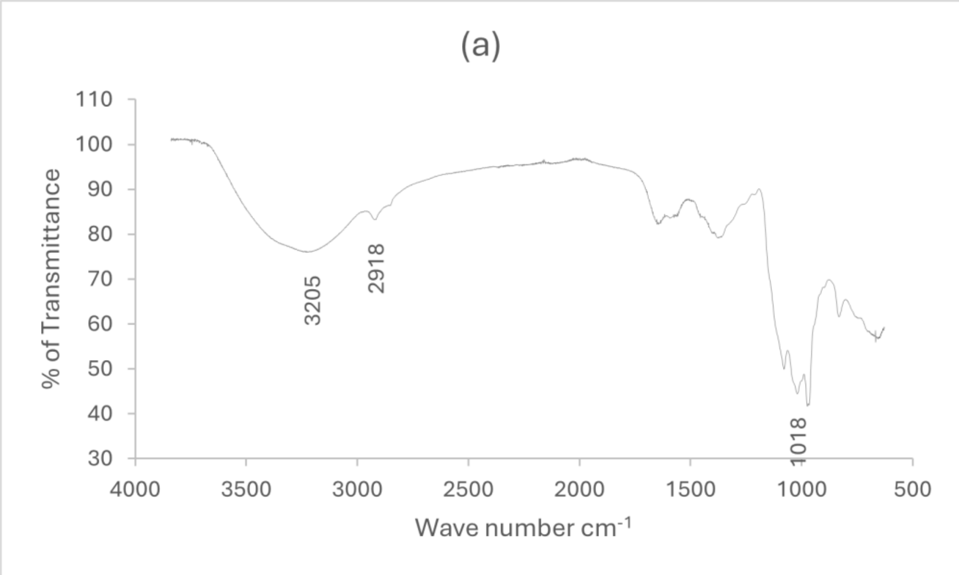

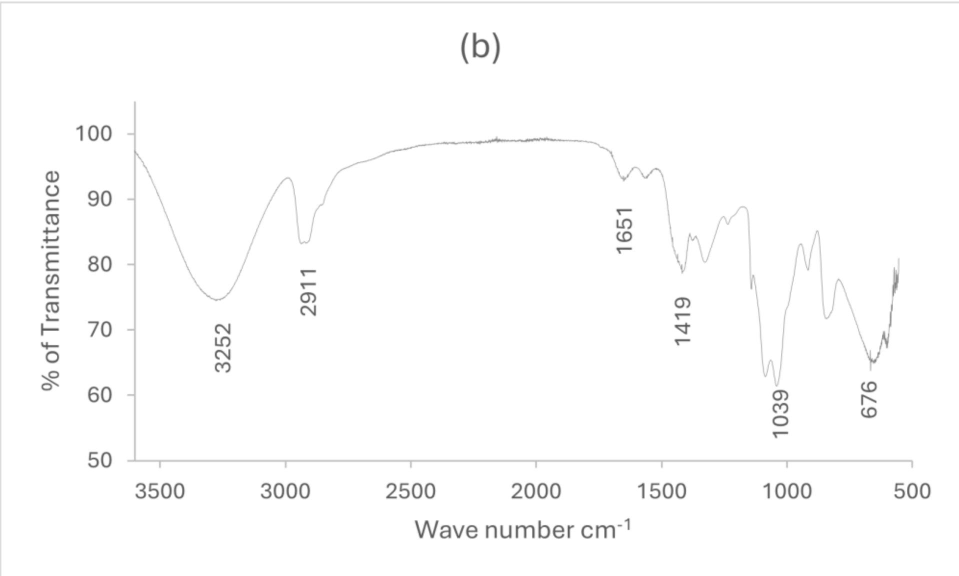

Figure 1. FT-IR spectra of (a) wheat bran extracted arabinoxylan, (b) WBAX 1:2:1 bioplastic.

3.2. Mechanical Properties

Tensile stress (TS) and elongation at break (EAB) are essential indicators of a film's mechanical performance, reflecting its ability to maintain structural integrity under applied stress. The wheat bran extracted arabinoxylan-based bioplastic films of different ratios (WBAX) demonstrated stress at break ranging from 1.2 MPa to 3.34 MPa and an elongation at break (EAB) across from 66% to 281% (Figure 2). The relatively higher stress values were attributed to the strong interactions between arabinoxylan, polyvinyl alcohol, and glycerol, as a plasticizer and reinforcing agent, thereby enhancing its rigidity and structural stability. However, among the four different bioplastic compositions, the WBAX bioplastic obtained from a matrix blend ratio of 1:2:1 showed the best mechanical performance, with a stress at break of 3.34 MPa and an EAB of 137%. This performance is comparable to that of low-density polyethylene (LDPE) and cotton fiber-based bioplastics [35].

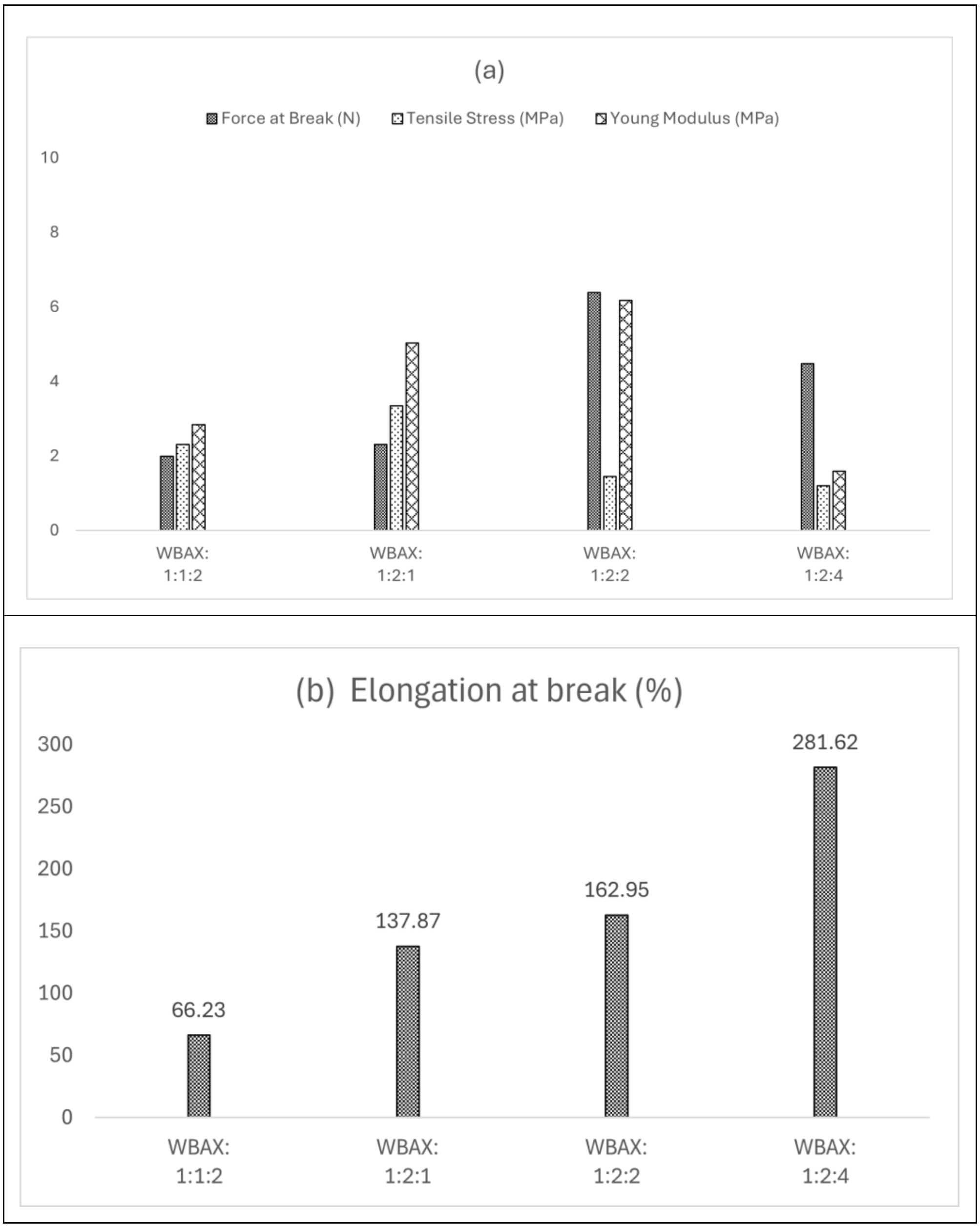

Figure 2. Mechanical properties of WBAX bioplastic at different ratios.

3.3. Scanning Electron Microscope (SEM) Analysis

Figure 3 shows the surface morphology of WBAX 1:2:1 bioplastic at two different resolutions. The SEM image displays the smooth surface of the bioplastic, although it contains some micro-voids. These micro-voids are due to the degree of glycerol dispersion within the plastic matrix. During the gelatinization process, the hydrogen bonds in the long arabinoxylan chains break down, allowing water molecules to penetrate the hydroxyl groups of the arabinoxylan, resulting in the formation of voids and micro-voids. The surface morphology of this bioplastic is found to be similar to the morphology of the polyethylene elastic material studied by Gere et al [36].

Preprints.org (www.preprints.org) | NOT PEER-REVIEWED | Posted: 18 June 2025 doi:10.20944/preprints202506.1515.v1

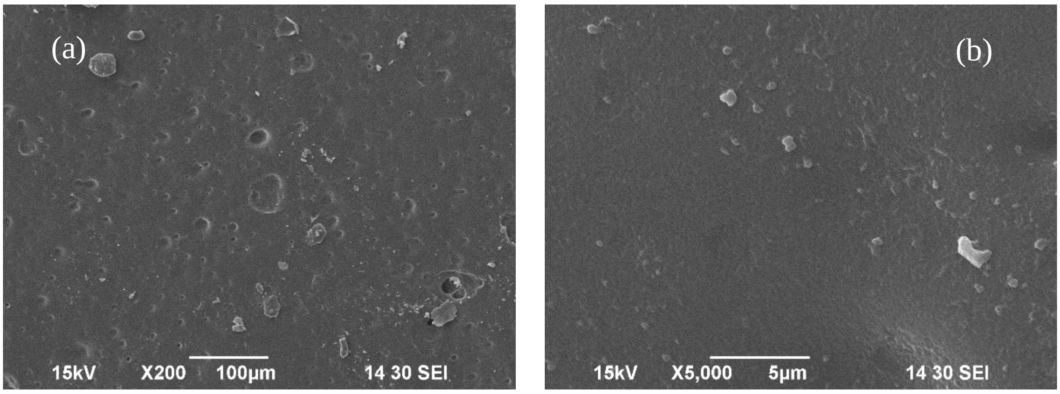

Figure 3. SEM image of (a) WBAX 1:2:1 bioplastic at 200x resolution, (b) WBAX 1:2:1 bioplastic at 5,000x resolution.

3.4. Film's Transparency

Table 2 shows that the bioplastic films exhibited lower transparency compared to synthetic polyethylene, which may be due to the presence of fillers and the integral thickness of the bioplastic films. Nonetheless, the PAV-based bioplastic demonstrated superior transparency relative to results reported in previous studies. For instance, Mulyono et al [24] reported a maximum transparency value of 3.13 for tapioca-based films, whereas the bioplastic films developed in this study achieved a transparency value of 1.50.

Table 2. Transparency of bioplastic films.

Film type	Absorbance	Transmission%	Thickness	Transparency
WBAX bioplastic film	1.23	5.92	0.19	1.50
CPS bioplastic film	1.25	5.60	0.17	1.52
Ziploc plastic bag	0.05	89.23	0.02	3.57
Walmart plastic bag	-	-	-	3.78
tapioca-based films,	-	-	-	3.13

3.5. Water Contact Angle

Figure 4 illustrates the water contact angle measurements, accompanied by images of water droplets on the surfaces of the film samples. Table 3 presents the water contact angle (WCA) values of the bioplastic film developed in this study, alongside those of a commercially available synthetic plastic bag and selected literature references [37]. The results indicate that the WBAX bioplastic film exhibits a water contact angle comparable to that of the market plastic, suggesting similar surface wettability characteristics. However, the WCA value of the WBAX bioplastic film remains below 90^0, indicating that it is not truly hydrophobic. For a material to be classified as hydrophobic, its water contact angle must exceed 90°. Therefore, while the WBAX film demonstrates reduced water affinity relative to other bioplastics, it does not meet the threshold for hydrophobicity, implying potential applications where moderate water resistance is sufficient.

Table 3. Water Contact Angle (WCA) of different plastics.

Film type	Water Contact Angle (degree)
WBAX bioplastic film	75.80
Ziploc plastic bag	124.83
Walmart plastic bag	76.78
PLA/starch/lecithin film	59.250

Preprints.org (www.preprints.org) | NOT PEER-REVIEWED | Posted: 18 June 2025 doi:10.20944/preprints202506.1515.v1

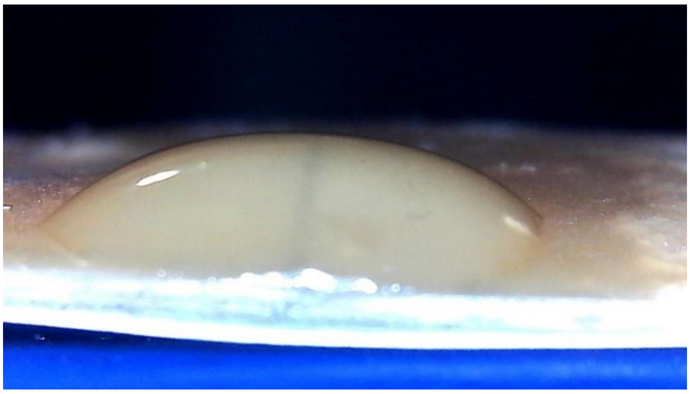

(a)

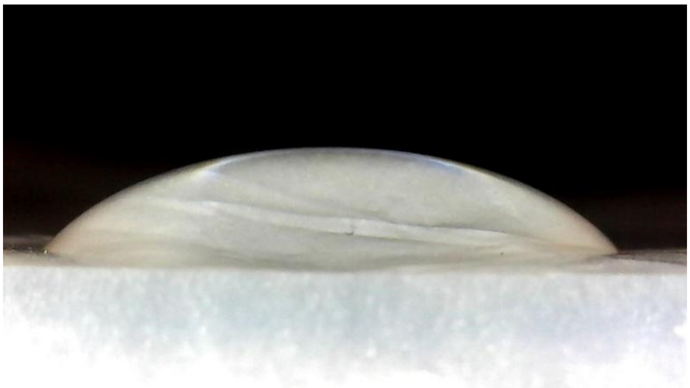

(b)

(c)

Figure 4. Water Contact Angle of (a) WBAX 1:2:1 bioplastic, (b) Walmart plastic bag, (c) Ziploc plastic bag.

3.6. Effect of Acids

The concentration of sulfuric acid has an impact on the weight loss behavior of the bioplastic produced from wheat bran-extracted arabinoxylan. As shown in Figure 5(a), weight loss increased when the acid concentration was raised from 10% to 20%, indicating that degradation depends on the acid content. At higher concentrations of 30% and 40%, the bioplastic showed complete

Preprints.org (www.preprints.org) | NOT PEER-REVIEWED | Posted: 18 June 2025 doi:10.20944/preprints202506.1515.v1

dissolution, dissolving almost entirely after 2 days in 30%, 40% acid, and after 4 days in 20%. However, in both cases, some residue remained, which makes the solution thicker and slurry, as shown in Figure 5 (b), indicating that the material did not completely break down. This suggests that high acid concentrations lead to severe degradation, possibly through extensive hydrolysis and disruption of the polymer matrix.

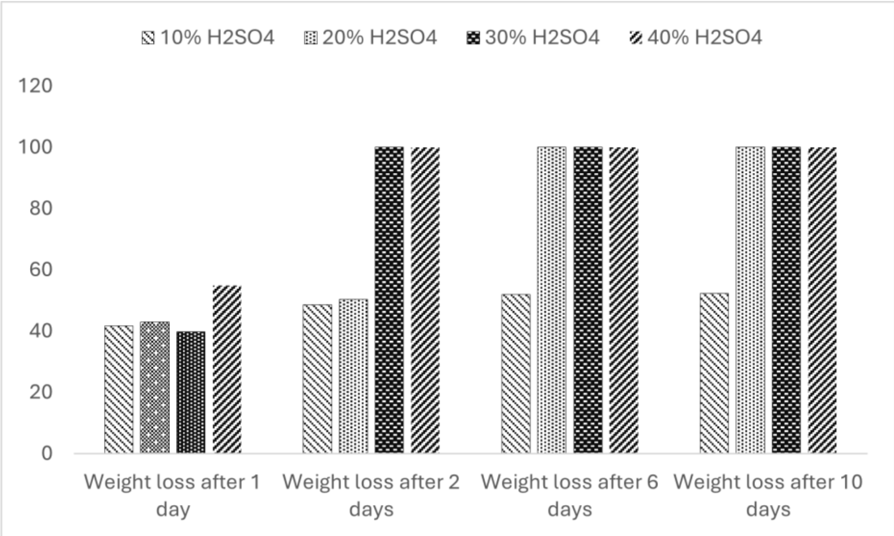

(a)

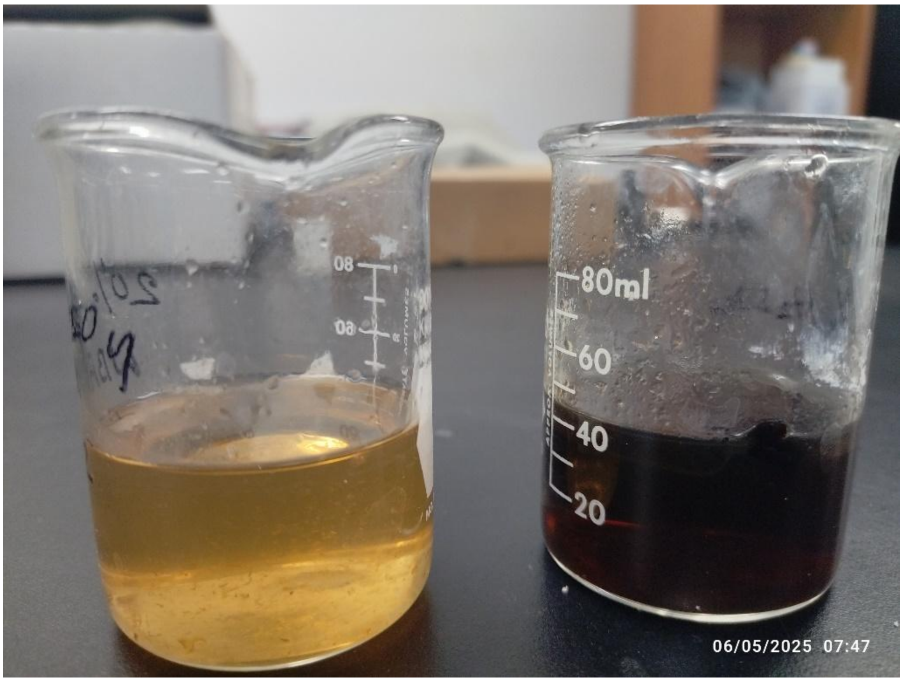

(b)

Figure 5. (a) Effect of acid concentration and treatment duration on weight loss, (b) the thicker and slurry solution after 2 days of dissolution (right side), 40% acid solution (left side).

In general, the bioplastics derived from wheat bran-extracted arabinoxylan exhibited strong resistance to acidic conditions at low concentration. Their acid resistance was slightly superior to that of commercial cellulose acetate (CA), which has an environmental resistance factor of three for strong

Preprints.org (www.preprints.org) | NOT PEER-REVIEWED | Posted: 18 June 2025 doi:10.20944/preprints202506.1515.v1

acids, classified as good resistance. This suggests that the bioplastics developed from this study not only offer a sustainable alternative but also performed comparably, if not better, in harsh chemical environments.

3.7. Effect of Alkalis

Figure 6 shows the weight loss behavior of bioplastic, produced from wheat bran-extracted arabinoxylan, when treated with different concentrations of potassium hydroxide (KOH) for ten days. After 10 days of exposure to a 40% sodium hydroxide solution, the maximum weight loss was 52% for WBAX 1:2:1 bioplastic for 10% KOH.

In comparison, with a 40% KOH concentration, both residues showed a lower weight loss of 31%. The results indicate that the alkali-resistant synthesized bioplastic is nearly identical. However, the bioplastics from this study exhibit strong resistance to alkalis when compared to commercial CA [32], which has a higher resistance factor (=3) against strong alkalis.

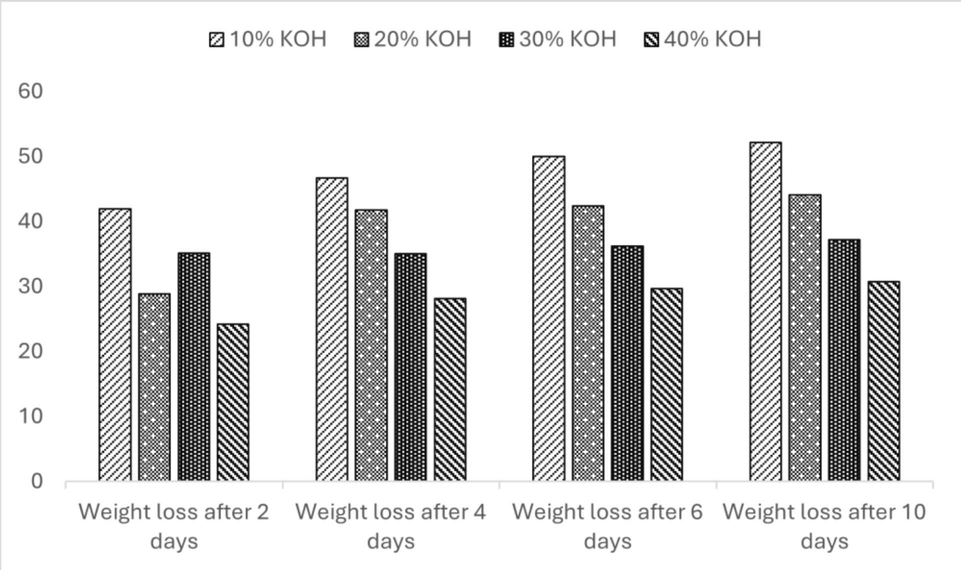

Figure 6. Effect of alkali concentration and treatment duration on weight loss.

3.8. Water Absorption Percentage

Film water absorption tendency indicates the presence of hydrophilic components in the material. Figure 7(a) illustrates the water absorption characteristics of the bioplastic film. The bioplastic film's increased water absorption is due to the presence of PVA, which has water-absorbing qualities. In contrast, those films exhibited a lower tendency, indicating the strong intermolecular forces and cross-linking within the matrix, limiting their interaction with water. Consequently, the bioplastic film at a 1:2:4 ratio displayed the lowest water solubility, while the film at a 1:2:1 proportion showed a moderate level of solubility.

Figure 7(b) illustrates the water solubility behavior of the bioplastic films. Among the tested formulations, the WBAX film with a 1:2:1 ratio exhibited the lowest water absorption, with solubility below 40%. In contrast, the film with a 1:2:4 ratio demonstrated the highest solubility, reaching approximately 70%. The reduced solubility observed in the 1:2:1 film suggests stronger intermolecular interactions and a more compact polymer matrix, which limits water penetration and absorption.

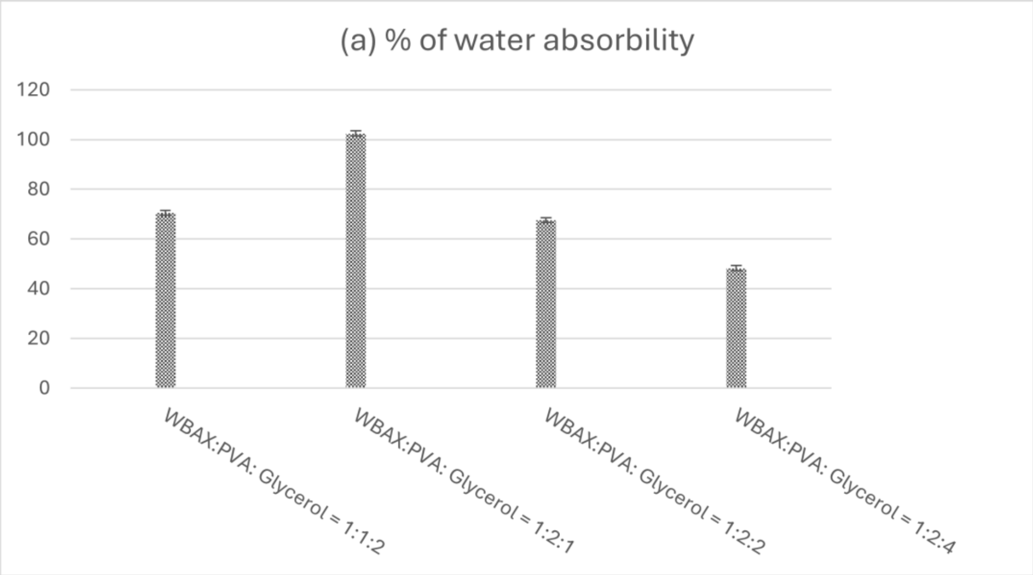

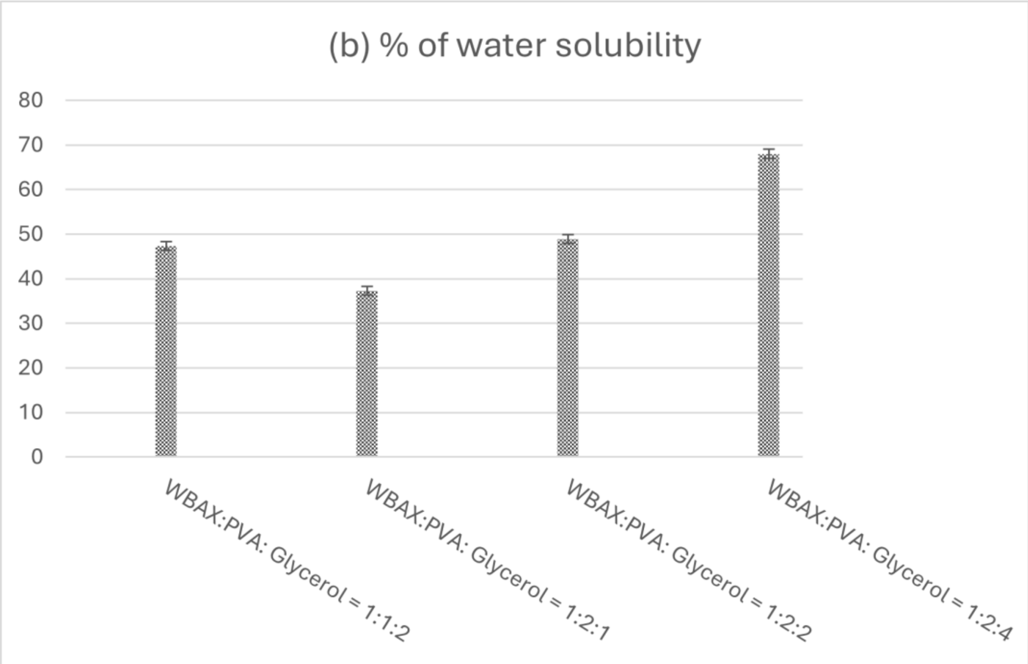

Figure 7. Water Absorption property of WBAX bioplastics (a) % of water absorbability, (b) % of water solubility.

3.9. Biodegradability Analysis

The biodegradability of the WBAX bioplastic film was evaluated through a soil burial testing for two months, and the structural changes were analyzed using Scanning Electron Microscopy (SEM) and Fourier Transform Infrared Spectroscopy (FT-IR). In Figure 8 (a,b,c,d), the SEM micrographs revealed notable morphological changes on the film surface after degradation. Compared to the smooth and uniform structure of the undegraded film, the buried samples exhibited cracks, voids, and surface erosion, indicating microbial and environmental activity that contributed to the breakdown of the polymer matrix.

These surface disruptions are characteristic of ongoing biodegradation, where microbial enzymes and soil moisture gradually weaken the film structure. The presence of micro-voids supports the hypothesis that biodegradation initiates through localized enzymatic attack, which leads to fragmentation of the polymer chains and structural disintegration. The physical appearance of the bioplastic film before and after degradation has been displayed in Figure 8 (e,f).

 doi:10.20944/preprints202506.1515.v1

Further confirmation of chemical degradation was obtained through FT-IR analysis. Figure 9 shows a comparison of spectra before and after the two-month burial period, revealing significant changes in peak intensities, reflecting the breakdown of functional groups. Most notably, the absorption peak below 1000 cm^{-1}, which corresponds to the hydrogen bonding among the matrix blend, disappeared entirely after degradation. The disappearance of these peaks indicates molecular degradation (hydrogen bond disruption) during the biodegradation process.

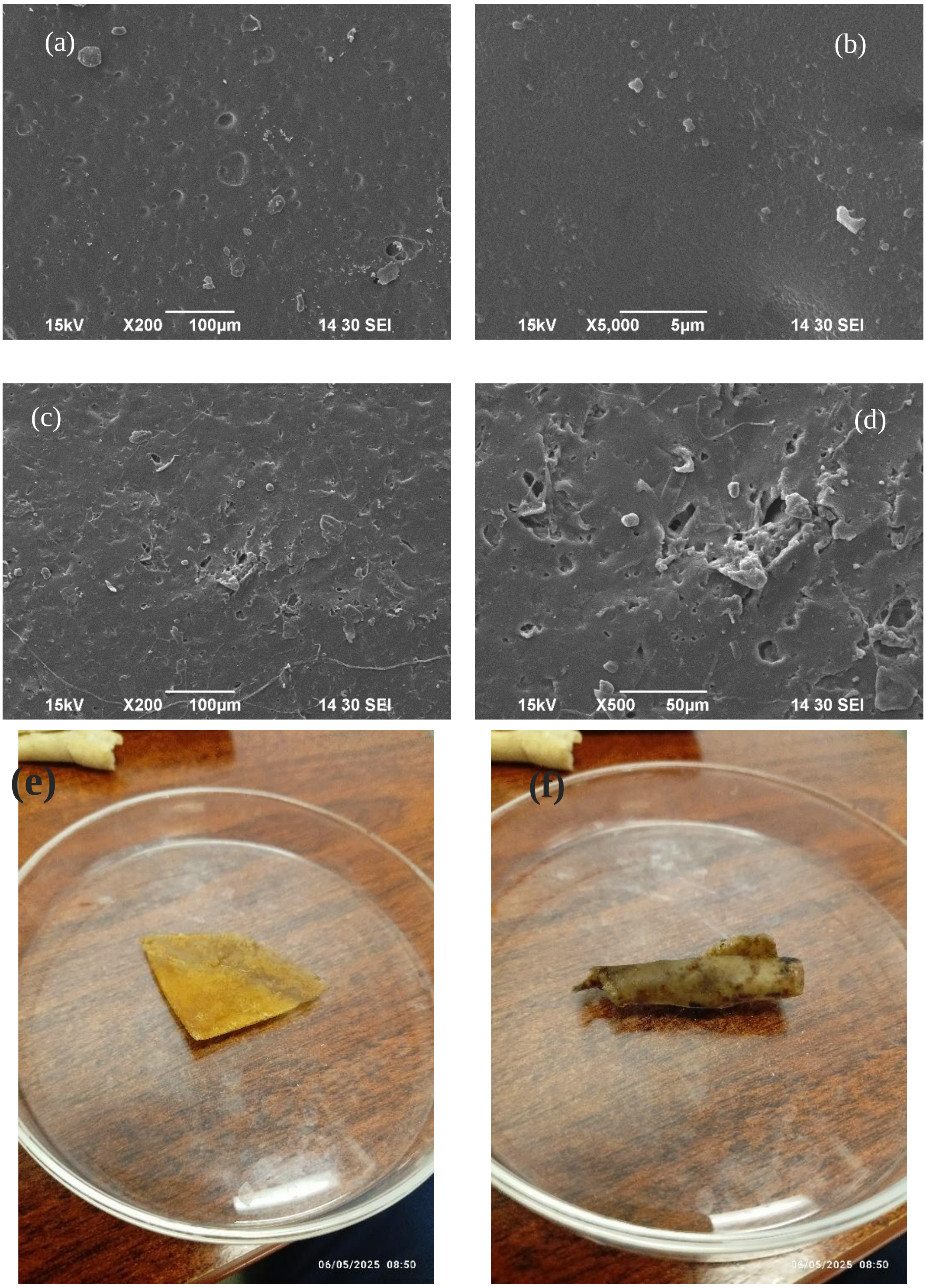

Figure 8. SEM image of (a) WBAX 1:2:1 before degradation at 200x resolution, (b) WBAX 1:2:1 before degradation at 500x resolution, (c) WBAX 1:2:1 after 2 months of natural degradation at 00x resolution, (d) WBAX 1:2:1 after 2 months of natural degradation at 500x resolution, (e) physical appearance of WBAX 1:2:1 before degradation, (f) physical appearance of WBAX 1:2:1 after degradation.

Preprints.org (www.preprints.org) | NOT PEER-REVIEWED | Posted: 18 June 2025 doi:10.20944/preprints202506.1515.v1

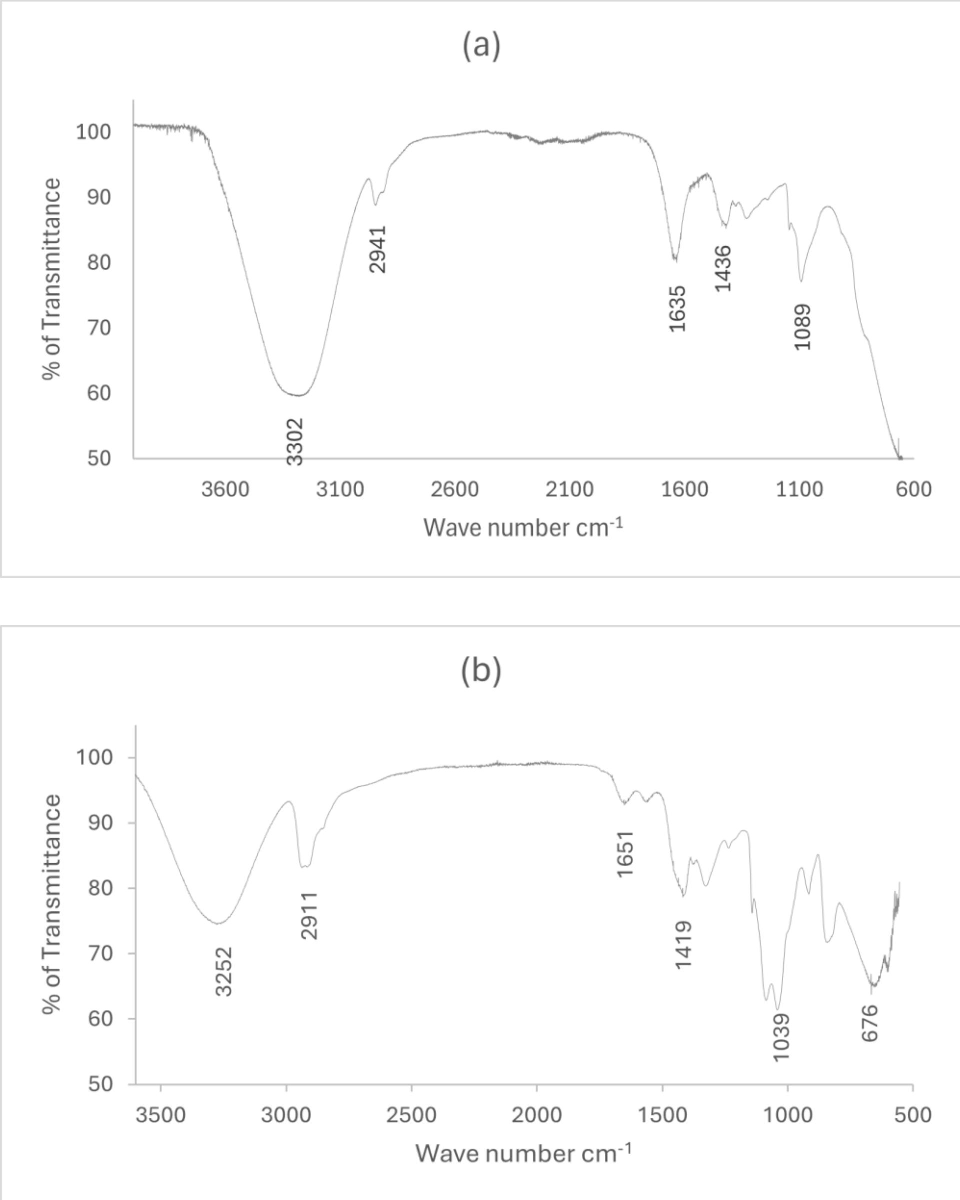

Figure 9. FT-IR spectra of (a) WBAX 1:2:1 bioplastic after 2 months of degradation, (b) WBAX 1:2:1 bioplastic before degradation.

4. Discussion

The wheat bran-extracted arabinoxylan-based bioplastic film produced in this study demonstrates a promising combination of mechanical strength, flexibility, chemical resistance, and environmental sustainability, making it a feasible alternative to conventional synthetic plastics, mainly low-density polyethylene (LDPE), which is excessively used in packaging applications worldwide [38].

Mechanically, WBAX bioplastic shows a tensile strength of 3.34 MPa, which are below the range of commercial LDPE, typically reported to have tensile strengths between 10–30 MPa and an elongation at break of 138%, which are well within the range of commercial LDPE, typically reported to have elongation values from 100% to 600%, depending on processing conditions [39]. This indicates that WBAX bioplastic could serve well in applications requiring flexibility and moderate mechanical performance, such as food packaging, and others.

Surface wettability analysis shows that WBAX bioplastic has a water contact angle (WCA) of 80°, indicating moderate hydrophilicity. In contrast, LDPE typically has a WCA greater than 95°, making it more hydrophobic [40]. Although this bioplastic film does not reach the hydrophobic threshold (>90°), its surface properties suggest reduced water affinity, sufficient for many short-term or controlled moisture exposure applications.

The water solubility of WBAX is approximately 40%, emphasizing its partial water resistance while allowing for biodegradation. In comparison, LDPE is virtually insoluble in water and highly resistant to biodegradation, contributing to its long-term environmental persistence [41]. The biodegradability of WBAX bioplastic is a significant environmental advantage, aligning with the growing demand for sustainable materials.

In terms of chemical resistance, WBAX biofilms show resilience in low concentrations of acid and high concentrations of alkali, supporting their use in chemically variable environments such as agriculture or food packaging. Additionally, the transparency of this biofilm enhances its suitability for applications where visibility or product presentation is significant. Table 4 shows the comparison of WBAX bioplastic with conventional synthetic plastic.

In conclusion, WBAX bioplastic films show modest performance in terms of mechanical and optical properties while extending the key benefit of environmental compatibility. Although somewhat more hydrophilic than LDPE, their biodegradable and partial water resistance make them suitable for applications where plastic waste reduction is a priority. Future improvements could focus on enhancing hydrophobicity through surface modifications or polymer blending, further expanding their application scope.

Table 4. Comparison of physico-mechanical properties of WBAX bioplastic and LDPE.

Property	WBAX Bioplastic	LDPE (Synthetic Plastic)
Tensile Strength (MPa)	3.34	10–30
Elongation at Break (%)	138	100–600
Water Contact Angle (°)	80	>95
Water Solubility (%)	~40	<1
Biodegradability	Yes	No
Acid Resistance	Low concentration	Moderate
Alkali Resistance	High concentration	Moderate
Transparency	Yes	Yes

5. Conclusions

The eco-friendly, arabinoxylan-based bioplastic derived from wheat bran was successfully synthesized through a multi-step procedure and characterized using a range of analytical techniques and environmental performance evaluations. In terms of mechanical performance, flexibility, optical property, and hydrophobicity, the WBAX bioplastic film in a 1:2:1 blend ratio performs the best, which is comparable to those of LDPE and other biodegradable plastics developed by several researchers. This bioplastic has high resistance to alkali and diluted mineral acid solutions, alongside showing moderate hydrophobicity. The bioplastics show excellent potential for biodegradation, emphasizing their environmental benefits over conventional petroleum-based plastics. Their ability to break down efficiently in natural environments significantly reduces the long-term environmental impact. The satisfactory overall performance of these bioplastics implied potential applications in packaging, food storage containers, and plastic tools, making them a promising alternative to conventional petroleum-based non-biodegradable materials.

6. Patents

 doi:10.20944/preprints202506.1515.v1

This section is not mandatory but may be added if there are patents resulting from the work reported in this manuscript

Author Contributions: The experiment was performed, and the manuscript was prepared by M.A.R.B. under the supervision of K.H., M.K., and K.H. and C. U were involved in concept creation. All authors have read and agreed to the published version of the manuscript.

Funding: This research was conducted at Mayville State University, Mayville, ND, with partial support from the NSF ND EPSCoR ND-ACES program (OIA #1946202). .

Institutional Review Board Statement: Not applicable.

Data Availability Statement: The original contributions presented in this study are included in the article. Further inquiries can be directed to the corresponding author.

Acknowledgments: The author gratefully acknowledges the support and facilities provided by the NDSU Electron Microscopy Core, which significantly contributed to the characterization aspects of this research. This material is based upon work supported by the National Science Foundation under Grant No. 0619098. We acknowledge the Department of Chemistry, UND, and Mechanical Engineering department NDSU for their contribution to the characterization aspect of this research.

Conflicts of Interest: The authors declare no conflicts of interest.

Abbreviations

The following abbreviations are used in this manuscript:

CA	Cellulose acetate
EAB	Elongation at break
FT-IR	Fourier Transform Infrared Spectroscopy
LDPE	Low-density polyethylene
PVA	Polyvinyl alcohol
SEM	Scanning Electron Microscope
TS	Tensile strength
WCA	Water contact angle
WB	Wheat bran
WBAX	Wheat bran arabinoxylan

References

1. Otoni, C. G.; Avena-Bustillos, R. J.; Azeredo, H. M. C.; Lorevice, M. V.; Moura, M. R.; Mattoso, L. H. C.; McHugh, T. H. Recent Advances on Edible Films Based on Fruits and Vegetables-A Review. *Comprehensive Reviews in Food Science and Food Safety* **2017**, *16* (5), 1151–1169. https://doi.org/10.1111/1541-4337.12281
2. Bayer, I. S.; Guzman-Puyol, S.; Heredia-Guerrero, J. A.; Ceseracciu, L.; Pignatelli, F.; Ruffilli, R.; Cingolani, R.; Athanassiou, A. Direct Transformation of Edible Vegetable Waste into Bioplastics. *Macromolecules* **2014**, *47* (15), 5135–5143. https://doi.org/10.1021/ma5008557.
3. Merino, D.; Paul, U. C.; Athanassiou, A. Bio-Based Plastic Films Prepared from Potato Peels Using Mild Acid Hydrolysis Followed by Plasticization with a Polyglycerol. *Food Packaging and Shelf Life* **2021**, *29*, 100707. https://doi.org/10.1016/j.fpsl.2021.100707.
4. Merino, D.; Simonutti, R.; Perotto, G.; Athanassiou, A. Direct Transformation of Industrial Vegetable Waste into Bioplastic Composites Intended for Agricultural Mulch Films. *Green Chemistry* **2021**, *23* (16), 5956–5971. https://doi.org/10.1039/d1gc01316e.
5. EUBIO_Admin. *Materials*. European Bioplastics e.V. https://www.european-bioplastics.org/bioplastics/materials/. (accessed April 20, 2024)
6. Aristei, L.; Villani, L.; Ricciardi, W. Directive . The Need to Raise Awareness on Plastic Misuse and Consequences on Health. *European Journal of PublicHealth* **2020**, *30*. https://doi.org/10.1093/eurpub/ckaa166.138.

7. Rudra, S. G., Nishad, J., Jakhar, N., & Kaur, C. Food industry waste: mine of nutraceuticals. *Int. J. Sci. Environ. Technol* **2015,** *4*(1), 205-229.
8. Addai, Z. R.; Abdullah, A.; Mutalib, S. A.; Musa, K. H. Evaluation of Fruit Leather Made from Two Cultivars of Papaya. *Italian Journal of Food Science* **2016**, *28* (1), 73–82. https://doi.org/10.14674/1120-1770/ijfs.v460.
9. Chen, J.; Tang, C.; Yue, Y.; Qiao, W.; Hong, J.; Kitaoka, T.; Yang, Z. Highly Translucent All Wood Plastics via Heterogeneous Esterification in Ionic Liquid/Dimethyl Sulfoxide. *Industrial Crops and Products* **2017**, *108*, 286–294. https://doi.org/10.1016/j.indcrop.2017.06.054.
10. Dai, H.; Chang, P. R.; Yu, J.; Geng, F.; Ma, X. Relationship of Thermoplastic Starch Crystallinity to Plasticizer Structure. *Starch - Stärke* **2010**, *62* (2), 86–89. https://doi.org/10.1002/star.200900189.
11. Khan, Z. A.; Butt, A. A.; Alghamdi, T. A.; Fatima, A.; Akbar, M.; Ramzan, M.; Javaid, N. Energy Management in Smart Sectors Using Fog Based Environment and Meta-Heuristic Algorithms. IEEE Access **2019**, 7, 157254–157267. https://doi.org/10.1109/access.2019.2949863.
12. Awika, J. M.; Vieno Piironen; Bean, S.; American Chemical Society. Division Of Agricultural and Food Chemistry. Advances in Cereal Science : Implications to Food Processing and Health Promotion; American Chemical Society: Washington, Dc, 2011.
13. Hensel, G.; Kastner, C.; Oleszczuk, S.; Riechen, J.; Kumlehn, J. *Agrobacterium*-Mediated Gene Transfer to Cereal Crop Plants: Current Protocols for Barley, Wheat, Triticale, and Maize. *International Journal of Plant Genomics* **2009**, *2009*, 1–9. https://doi.org/10.1155/2009/835608
14. Hemery, Y.; Rouau, X.; Lullien-Pellerin, V.; Barron, C.; Abecassis, J. Dry Processes to Develop Wheat Fractions and Products with Enhanced Nutritional Quality. Journal of Cereal Science **2007**, 46 (3), 327–347. https://doi.org/10.1016/j.jcs.2007.09.008.
15. Sarker, N. C.; Rahim, A.; Hillukka, G.; Holter, B.; Kjelland, M.; Hossain, K. Pyrolyzed Biochar from Agricultural Byproducts: Synthesis, Characterization, and Application in Water Pollutants Removal. *Processes* **2025**, *13* (5), 1358–1358. https://doi.org/10.3390/pr13051358.
16. Chen, Z.; Mense, A. L.; Brewer, L. R.; Shi, Y.-C. Wheat Bran Layers: Composition, Structure, Fractionation, and Potential Uses in Foods. *Critical Reviews in Food Science and Nutrition* **2023**, 1–24. https://doi.org/10.1080/10408398.2023.2171962.
17. Katileviciute, A.; Plakys, G.; Budreviciute, A.; Onder, K.; Damiati, S.; Kodzius, R. A Sight to Wheat Bran: High Value-Added Products. *Biomolecules* **2019**, *9* (12), 887. https://doi.org/10.3390/biom9120887
18. Kaya, K.; Pehlivan, E.; Schmidt, C.; Bahadir, M. Use of Modified Wheat Bran for the Removal of Chromium(VI) from Aqueous Solutions. *Food Chemistry* **2014**, *158*, 112–117. https://doi.org/10.1016/j.foodchem.2014.02.107.
19. Attallah, O. A.; Mojicevic, M.; Garcia, E. L.; Azeem, M.; Chen, Y.; Asmawi, S.; Brenan Fournet, M. Macro and Micro Routes to High Performance Bioplastics: Bioplastic Biodegradability and Mechanical and Barrier Properties. *Polymers* **2021**, *13* (13), 2155. https://doi.org/10.3390/polym13132155
20. Luc Avérous; Pollet, E. *Environmental Silicate Nano-Biocomposites*; London Springer London, 2012.
21. Hossain, A.; Mahmud, M.; Koistinen, K.; Davisson, G.; Roeges, B.; Boechler, H.; Md Abdur Badsha; Khan, R.; Kjelland, M.; Dorsa Fereydoonpour; Quadir, M.; Mallik, S.; Hossain, K. Wheat Bran Polymer Scaffolds: Supporting Triple-Negative Breast Cancer Cell Growth and Development. **2025**. https://doi.org/10.20944/preprints202505.1194.v1.
22. Mendes, J. F.; Laís Bruno Norcino; Anny Manrich; Carla, A.; Oliveira, J. E.; Luiz. Development, Physical-Chemical Properties, and Photodegradation of Pectin Film Reinforced with Malt Bagasse Fibers by Continuous *Casting*. *Journal of Applied Polymer Science* **2020**, *137* (39). https://doi.org/10.1002/app.49178.
23. Nurul Nadiah Azmi; Mohd; Noor, S.; Mahmud, J. Testing Standards Assessment for Silicone Rubber. *2014 International Symposium on Technology Management and Emerging Technologies* **2014**. https://doi.org/10.1109/istmet.2014.6936529.
24. Mulyono, N., Suhartono, M.T. and Angelina, S., 2015. Development of Bioplastic Based on Cassava Flour and Its Starch Derrivatives for Food Packaging. *Journal of Harmonized Research in Applied Sciences*, 3(2), pp.125-3

 doi:10.20944/preprints202506.1515.v1

25. Wang, B.; Duan, Y.; Xin, Z.; Yao, X.; Abliz, D.; Ziegmann, G. Fabrication of an Enriched Graphene Surface Protection of Carbon Fiber/Epoxy Composites for Lightning Strike via a Percolating-Assisted Resin Film Infusion Method. Composites Science and Technology 2018, 158, 51–60. https://doi.org/10.1016/j.compscitech.2018.01.047.
26. Baba, E. M.; Cansoy, C. E.; Zayim, E. O. Optical and Wettability Properties of Polymers with Varying Surface Energies. *Applied Surface Science* **2015**, *350*, 115–120. https://doi.org/10.1016/j.apsusc.2015.02.150.
27. Deng, R.; Shen, T.; Chen, H.; Lu, J.; Yang, H.-C.; Li, W. Slippery Liquid-Infused Porous Surfaces (SLIPSs): A Perfect Solution to Both Marine Fouling and Corrosion? *Journal of Materials Chemistry A* **2020**, *8* (16), 7536–7547. https://doi.org/10.1039/d0ta02000a.
28. Kumar, M.; Bhardwaj, R. Wetting Characteristics of Colocasia Esculenta (Taro) Leaf and a Bioinspired Surface Thereof. *Scientific Reports* **2020**, *10* (1). https://doi.org/10.1038/s41598-020-57410-2.
29. Liu, D.; Chen, P.; Mu, J.; Yu, Q.; Lu, C. Improvement and Mechanism of Interfacial Adhesion in PBO Fiber/Bismaleimide Composite by Oxygen Plasma Treatment. *Applied Surface Science* **2011**, *257* (15), 6935–6940. https://doi.org/10.1016/j.apsusc.2011.03.035.
30. Rasband, W. S. *ImageJ*. Nih.gov. https://imagej.nih.gov/ij/.
31. Saberi, B.; Chockchaisawasdee, S.; Golding, J. B.; Scarlett, C. J.; Stathopoulos, C. E. Physical and Mechanical Properties of a New Edible Film Made of Pea Starch and Guar Gum as Affected by Glycols, Sugars and Polyols. *International Journal of Biological Macromolecules* **2017**, *104*, 345–359. https://doi.org/10.1016/j.ijbiomac.2017.06.051.
32. Mostafa, N. A.; Farag, A. A.; Abo-dief, H. M.; Tayeb, A. M. Production of Biodegradable Plastic from Agricultural Wastes. *Arabian Journal of Chemistry* **2018**, *11* (4), 546–553. https://doi.org/10.1016/j.arabjc.2015.04.008.
33. Müller, R. Biodegradability of Polymers: Regulations and Methods for Testing. *Biopolymers Online* **2002**. https://doi.org/10.1002/3527600035.bpola012.
34. Harunsyah; Yunus, M.; Fauzan, R. Mechanical Properties of Bioplastics Cassava Starch Film with Zinc Oxide Nanofiller as Reinforcement. *IOP Conference Series: Materials Science and Engineering* **2017**, *210*, 012015. https://doi.org/10.1088/1757-899x/210/1/012015.
35. Rumi, S. S.; Liyanage, S.; Abidi, N. Conversion of Low-Quality Cotton to Bioplastics. *Cellulose* **2021**. https://doi.org/10.1007/s10570-020-03661-1.
36. Edhirej, A.; Sapuan, S. M.; Jawaid, M.; Zahari, N. I. Effect of Various Plasticizers and Concentration on the Physical, Thermal, Mechanical, and Structural Properties of Cassava-Starch-Based Films. *Starch - Stärke* **2016**, *69* (1-2), 1500366. https://doi.org/10.1002/star.201500366.
37. Sena, J.; Johannissen, L. O.; Blaker, J. J.; Hay, S. A Machine Learning Model for the Prediction of Water Contact Angles on Solid Polymers. *The Journal of Physical Chemistry B* **2025**. https://doi.org/10.1021/acs.jpcb.4c06608.
38. Marsh, K.; Bugusu, B. Food Packaging - Roles, Materials, and Environmental Issues. *Journal of Food Science* **2007**, *72* (3), R39–R55. https://doi.org/10.1111/j.1750-3841.2007.00301.x.
39. Andrady, A. L.; Neal, M. A. Applications and Societal Benefits of Plastics. *Philosophical Transactions of the Royal Society B: Biological Sciences* **2009**, *364* (1526), 1977–1984. https://doi.org/10.1098/rstb.2008.0304.
40. Bodas, D.; Khan-Malek, C. Hydrophilization and Hydrophobic Recovery of PDMS by Oxygen Plasma and Chemical Treatment—an SEM Investigation. *Sensors and Actuators B: Chemical* **2007**, *123* (1), 368–373. https://doi.org/10.1016/j.snb.2006.08.037.
41. Hopewell, J.; Dvorak, R.; Kosior, E. Plastics Recycling: Challenges and Opportunities. *Philosophical Transactions of the Royal Society B: Biological Sciences* **2009**, *364* (1526), 2115–2126. https://doi.org/10.1098/rstb.2008.0311.